

2015

Comparison of Lock-in and Pulse-Phase Thermography for Defect Characterization in FRP Composites Applied to Concrete

Jeff Brown

Embry-Riddle Aeronautical University, browj112@erau.edu

Sai Harsha Chittineni

Embry-Riddle Aeronautical University

Follow this and additional works at: <https://commons.erau.edu/publication>



Part of the [Civil and Environmental Engineering Commons](#), [Electromagnetics and Photonics Commons](#), and the [Materials Science and Engineering Commons](#)

Scholarly Commons Citation

Brown, J., & Chittineni, S. H. (2015). Comparison of Lock-in and Pulse-Phase Thermography for Defect Characterization in FRP Composites Applied to Concrete. *Thermosense: Thermal Infrared Applications XXXVII; Proceedings of SPIE Vol. 9485, 9485()*. <https://doi.org/10.1117/12.2177260>

This Conference Proceeding is brought to you for free and open access by Scholarly Commons. It has been accepted for inclusion in Publications by an authorized administrator of Scholarly Commons. For more information, please contact commons@erau.edu.

Comparison of lock-in and pulse-phase thermography for defect characterization in FRP composites applied to concrete

Jeff Brown^a and Sai Harsha Chittineni^b

Dept. of Civil Engineering^a, Embry-Riddle Aeronautical University, Daytona Beach, FL, 32114
Dept. of Aerospace Engineering^b, Embry-Riddle Aeronautical University, Daytona Beach, FL, 32114

ABSTRACT

Thermal imaging is a well-established technique for the non-destructive evaluation of FRP composites applied to reinforced concrete. Defect characterization using IR thermography, however, remains a topic of on-going research, and there are currently no universally accepted standards for data collection or interpretation. This research involved large scale thermography inspection of two FRP strengthened bridge girders that were removed from service after approximately 10 years of service in a potentially corrosive marine environment. Trial inspections were performed on test areas where defects could be identified using sounding methods. Two procedures showed the most promise for identifying and characterizing defects: sinusoidal (lock-in style) heating with periods ranging from 5 s to 40 s and constant step heating for 30 s followed by 60 s of cooling. Both methods resulted in a series of phase images that provided insight into the depth and general nature of detected defects. This paper presents the findings of a comparison study between these two thermal imaging techniques.

Keywords: Infrared thermography, nondestructive evaluation, FRP composites, repair of civil infrastructure

1. INTRODUCTION

The deterioration of roads and bridges in the U.S. continues to gain significant attention in the media. A *60 Minutes* report that aired on November 23, 2014, cited data from the Federal Highway Administration (FHWA) stating that “nearly 70,000 bridges in America—one out of every nine—is now considered to be structurally deficient.”¹ While the number of structurally deficient bridges in the U.S. is certainly alarming (61,365, or 10% of the National Bridge Inventory (NBI), as of December 2014²), the long-term trend appears to be heading in a more positive direction. Over the past 22 years, since 1992, the number of structurally deficient bridges in the U.S. has decreased by almost 51% from 124,072. The total percentage of the NBI classified as structurally deficient has also decreased from 21.7% in 1992 to 10% in 2014.

The past two decades have also seen an increase in the use of fiber-reinforced polymer (FRP) composites to strengthen existing bridges³. Two fundamental application types include (1) the repair of acute damage due to unexpected mishaps (e.g. impact damage by over height vehicles) and (2) extending the useful service life of a bridge suffering from chronic deterioration. For reinforced concrete structures, remediation of chronic deterioration often involves repairing damage caused by the corrosion of internal reinforcing steel. The FRP composite can be applied externally to the structure using a wet lay-up method in order to compensate for any section loss experienced by the reinforcement. The FRP also serves to protect the remaining internal reinforcing steel by preventing harmful chloride intrusion.

There are two fundamental concerns surrounding the performance and long-term durability of FRP composites used to strengthen civil infrastructure. First, strengthening for flexure and shear are considered “bond-critical” applications. It is important that these systems are installed correctly from the outset to ensure that anticipated tensile stresses are fully developed through a sound bond-line. Air-bubbles or voids between the composite and the concrete are generally considered to be detrimental to system performance. Acceptance criteria for FRP composite systems have been proposed by the American Concrete Institute⁴, ICC-ES⁵, and the National Cooperative Highway Research Program (NCHRP)³. These criteria establish acceptable limits for defect size as well as prescribe required steps for remediation if a defect is known to exist in the FRP system. For example, ACI 440.2R-08 states “Small delaminations less than 2 in² each are permissible as long as the delaminated area is less than 5% of the total laminate area and there are no more

than 10 such delaminations per 10 ft².” Large delaminations (> 25 in²) must be repaired by cutting away the damaged area and replacing the removed area with a new FRP patch. Finally, delaminations between 2 in² and 25 in² may be repaired either by resin injection or ply replacement, depending on the number of defects present and their location.

The second concern relates to the potential for ongoing corrosion after the externally bonded FRP system is applied. Internal concrete cracking in the longitudinal direction of the member can ultimately lead to concrete cover delamination. Maintaining concrete cover is critical for facilitating stress transfer into the composite system. Standard practice for repair of corrosion damage involves first removing all of the damaged or spalled concrete. The reinforcing steel is then cleaned to remove any scale or corrosion by-product. The original cross-section is then restored by forming the member with plywood and injecting a cementitious grout. Once the grout has cured, the FRP composite is applied in order to achieve the desired strengthening objectives. The objective of this repair process is to provide a fresh, chloride-free layer of cementitious material around the cleaned reinforcing steel. The addition of the FRP layer on the surface also protects the grout and prevents exposure to chlorides in harsh marine environments. There is the potential that the corrosion process may continue, and, if the reinforced concrete element is fully encapsulated by the FRP system, early warning signs (e.g. iron-oxide staining or minor cracking/spalling) may not be visible.

Thermal imaging has been studied extensively for its potential use as a non-destructive evaluation tool to identify defects in FRP composite systems applied to concrete⁶⁻¹⁰. Several issues, however, remain unresolved. Full-field deployment for in-service bridges presents numerous challenges regarding access and data collection. Also, there are no formalized methodologies for surface heating, image acquisition, and data post-processing that can be used to characterize detected defects. This research aims to answer basic questions surrounding full-field deployment and lay the initial groundwork for future standards.

2. PROJECT BACKGROUND AND OBJECTIVES

In 2011, the Florida Department of Transportation (FDOT) replaced a short relief bridge (total length = 216 ft) on the eastern side of the causeway carrying U.S. 192 over the Indian River in Brevard County, Florida. The concrete tee beam bridge was originally constructed in 1948 and then widened in 1969. In 1994, corrosion damage was evident in several spans, and the FDOT decided to repair the damaged girders with FRP composites (Figure 1). The first repair consisted of a uni-directional (0 degree) carbon FRP system. This repair was later replaced with a multi-layer 0/90 degree woven fabric system in 1999. When demolition began for the bridge replacement project in 2010, two of the FRP strengthened beams were kept in-tact for additional research and study at the FDOT Structures Research Center in Tallahassee, Florida.



Figure 1. Corrosion damage and 1994 repair of US 192 relief bridge over the Indian River in Brevard County, Florida.

A larger research project by the University of Florida and the Florida DOT to assess the load-carrying capacity of these FRP-strengthened girders is currently underway. Researchers from Embry-Riddle Aeronautical University were given the opportunity to perform an infrared thermography inspection of the FRP systems under laboratory conditions before and after load testing. Preliminary planning for this project revealed several fundamental questions that ultimately guided the direction of this thermography research:

1. What heating methods are appropriate for this specific FRP system?
2. Considering the overall surface area of the system (165 ft² for Beam 1 and 132 ft² for Beam 2), how much of the FRP system could be inspected in a reasonable period of time?
3. What level of defect characterization is appropriate for this type of inspection?

Very little historical information was available regarding the thickness and layout of the FRP systems that were applied to each beam in 1999. The thickness of the composite has been shown to have significant impact on the heating requirements and image acquisition parameters for a given infrared thermography protocol. Without a priori knowledge of FRP system characteristics, it is difficult to ensure that the thermal imaging parameters have been optimized. If the energy input is too low, or the observation period after heating is too short, deeper defects may be missed altogether. On the other hand, spending more time than necessary to inspect a specific area may make inspection of the entire system unpractical.

Several iterations were performed using different thermography inspection parameters on areas of the system containing defects that were easily detected using sounding methods. A decision was made to focus on two separate 3 ft² zones and compare the results for two commonly employed thermal imaging methods: lock-in thermography (LIT) and pulse-phase thermography (PPT). Research is currently ongoing that seeks to characterize the entire 297 ft² of composite that was applied to both beams.

3. EXPERIMENTAL PROGRAM

3.1 Test Setup

The surface of the composite was divided into 18 in zones along the length of each beam. The current study focused on two zones that were located on the side of Beam 1 with each zone measuring 18 in x 24 in. The field of view for the camera was approximately 24 in x 32 in in order to provide some overlap between sets of thermal images.

The heat source used for all IRT experiments was eight 500 W halogen lamps. An analog dimmer was used to control the output intensity, and the total surface area illuminated by the lamps was 24 in x 32 in (5.3 ft²). A FLIR A655 SC with a 480 x 640 pixel uncooled microbolometer array detector was used to record thermal images at a rate of 3 frames per second. A custom frame was constructed to hold the lamps at an appropriate stand-off distance and provide a stable support for the infrared camera. The configuration shown in Figure 3 was used to inspect the bottom surface of Beam 1. This configuration required six feet of clearance between the ground surface and the beam soffit. The beam was lowered and the lamps and camera were reconfigured in order to inspect the sides.

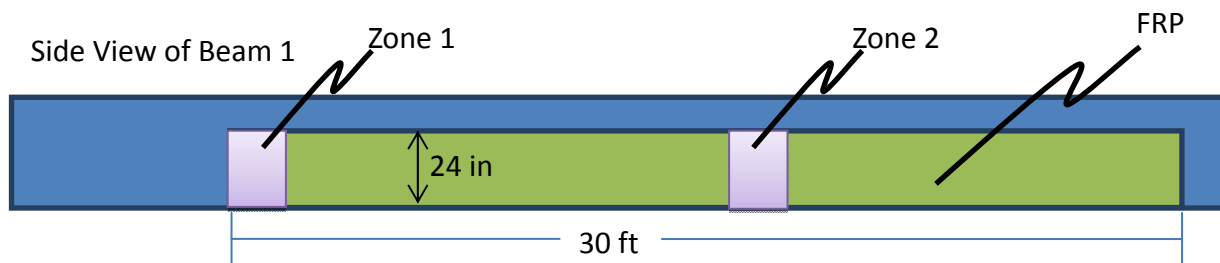


Figure 2. Zones of interest for current study. FRP composite applied to west side of Beam 1.



Figure 3. Heat lamp and IR camera configuration used for inspecting bottom surface of Beam 1.

3.2 Lock-in Thermography

The heating profile that was applied to each zone consisted of four, single-cycle sinusoids with the following periods:

- $T = 5$ s
- $T = 10$ s
- $T = 20$ s
- $T = 40$ s

The intensity of the lamps at time = 0 s for each cycle was 50% of the maximum. No cool down period was provided between cycles, which resulted in a total data acquisition period of 75 s for each zone. The series of images obtained for each of the four periods in the time domain was processed using a least-squares sinusoidal curve fit. The temperature vs. time response was extracted for each pixel over each period in order to obtain the corresponding phase shift. These phase shift values for each pixel were then reassembled into a total of 4 phase images (one for each period) for each zone.

Phase images for Zone 1 are provided in Figure 4. An initial observation is that the overall thickness of the FRP composite varies across the zone. The upper portion of Zone 1 consists of a single layer of woven FRP fabric (0.8 mm thick) while the lower portion consists of two layers. Because the phase response is sensitive to this detail of the FRP system at a period of 5 seconds, it is possible to deduce that any defects first appearing in phase images with $T = 5$ s occur beneath a single layer of FRP. Two defects, D1 and D2, are highlighted for discussion purposes. D1 first appears near the center in the $T = 5$ s image while D2 first appears near the bottom in the $T = 10$ s image. The general conclusion is that D1 lies between one layer of FRP and the concrete substrate while D2 lays beneath two layers of FRP between the composite and the concrete.

Similar results were obtained for Zone 2 (Figure 5). In addition to the two distinct regions of single and double-layer composite, these images also reveal an overlap shear splice that connects sheets running along the length of the beam. Defect D1 (lower left of $T = 5$ s phase image) occurs between the first and second layer of FRP while Defect D2 occurs under two layers of FRP at the FRP/concrete interface. Another interesting observation is that the peak intensity of the defect signal strength varies as a function of period for defects that occur at different depths. For example, the peak defect signal strength for D1 occurs in the $T = 10$ s image and then decreases as the period increases to 40 s. The defect signal strength for D2 is essentially zero in the $T = 5$ s image and then starts to develop in the $T = 10$ s image. Unlike

D1, the relative intensity of the phase shift with respect to the surrounding area for D2 continues to increase as the period increases to 40 s.

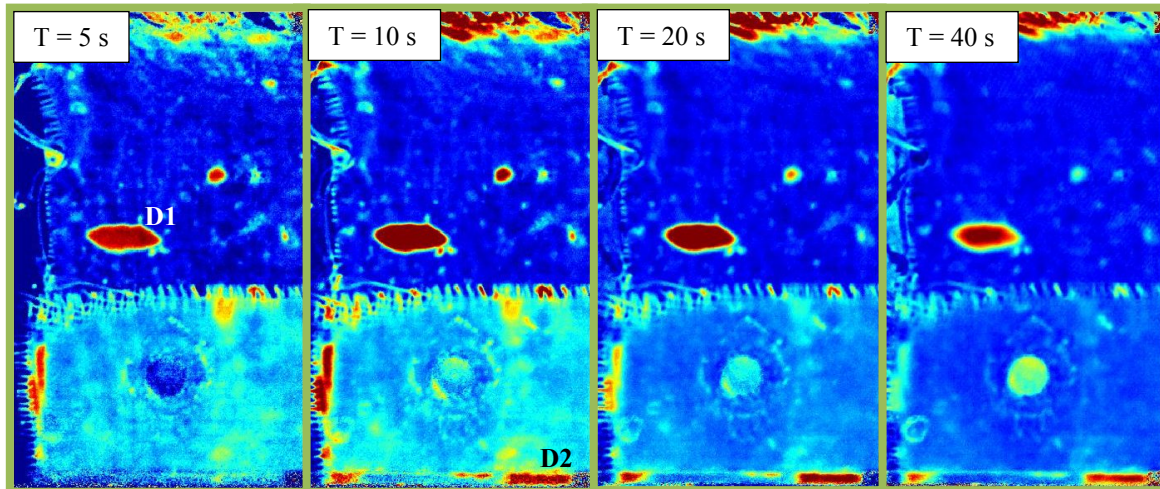


Figure 4. Lock-in Phase images for Zone 1 (west side of Beam 1).

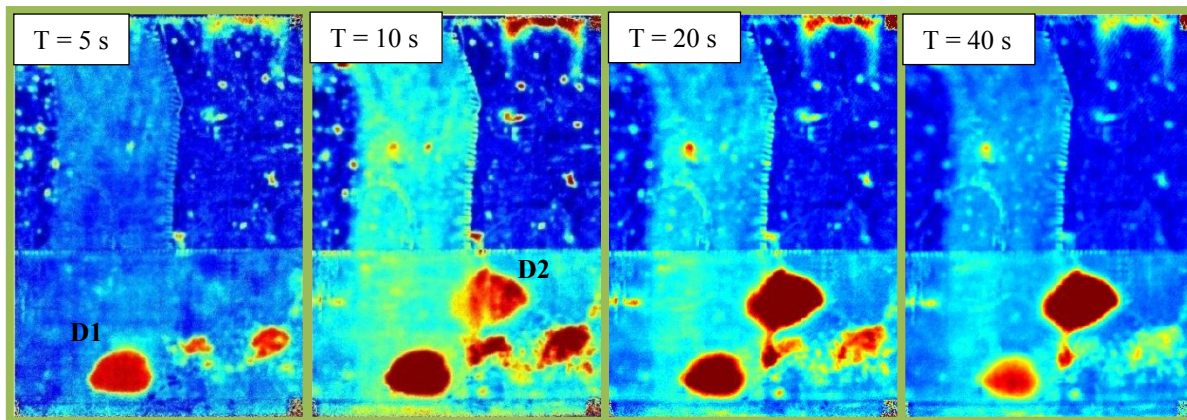


Figure 5. Lock-in Phase images for Zone 2 (west side of Beam 1).

3.3 Pulse Phase Thermography

Each zone was heated for 30 s at a constant intensity (maximum power to eight 500 W halogen lamps). Images were recorded at a rate of three frames per second for an additional 60 seconds while the surface cooled. This resulted in a total data acquisition period of 90 s. Only images collected during the cooling portion of the experiment were used in the pulse-phase thermography (PPT) analysis. A discrete Fourier transform was applied to the temperature vs. time history for each pixel extracted from the series of thermal images collected during cooling. The phase values obtained for each pixel were then reassembled into a series of phase images. The 181 thermal images resulted in a set of 90 unique phase images corresponding to a minimum frequency of 0.0167 Hz (1/60 s) and a maximum frequency of 1.5 Hz (half the sampling frequency, which was 3 Hz).

Typical PPT applications rely on surface heating from high-energy flash devices. This method may not be compatible with surface heating for areas on the order of 5 ft². As a result, lower intensity heat fluxes require a longer duration pulse in order to develop a sufficient defect signal strength. The 30 s heat pulse and 60 s cooling window chosen for the present study were somewhat arbitrary. Recent research by Mabry et al.¹¹ has explored the effect of pulse duration and truncation window time periods on PPT results; however, further analysis is needed to properly align their results with the current study.

Pulse Phase Thermography results for Zone 1 and Zone 2 are provided in Figure 6 and Figure 7, respectively. In an effort to remain consistent with the results format from the section on lock-in thermography, the frequency values from the DFT output have been converted into their corresponding periods by taking their reciprocals. It is important to note, however, that even though the reported periods are the same, the resulting phase images were obtained through fundamentally different approaches. PPT results for Zone 1 indicate that Defect D1 was detected. Data for Defect D2 was not available due to improper alignment of the IR camera.

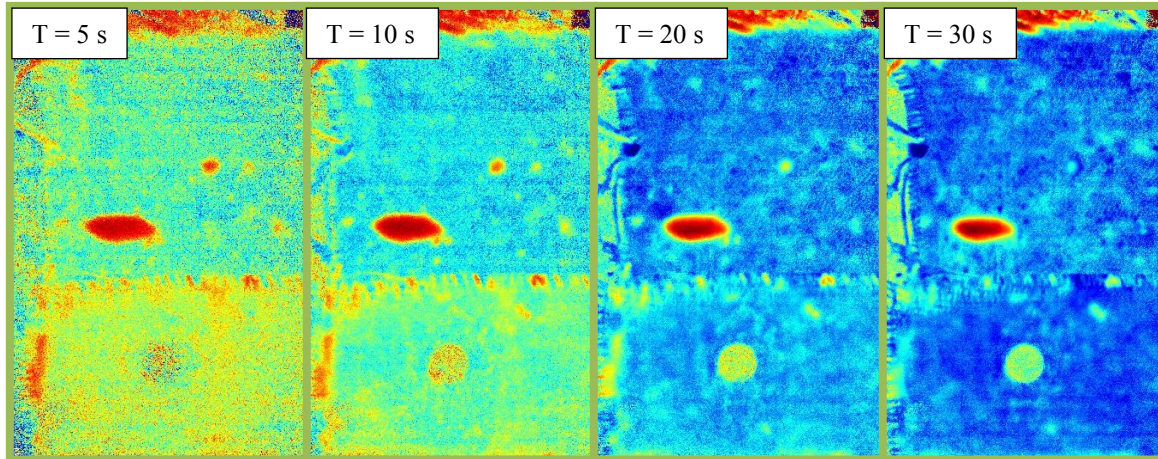


Figure 6. Pulse Phase images for Zone 1 (west side of Beam 1). Period, T , is equal to the inverse of the corresponding frequency from the discrete Fourier transform.

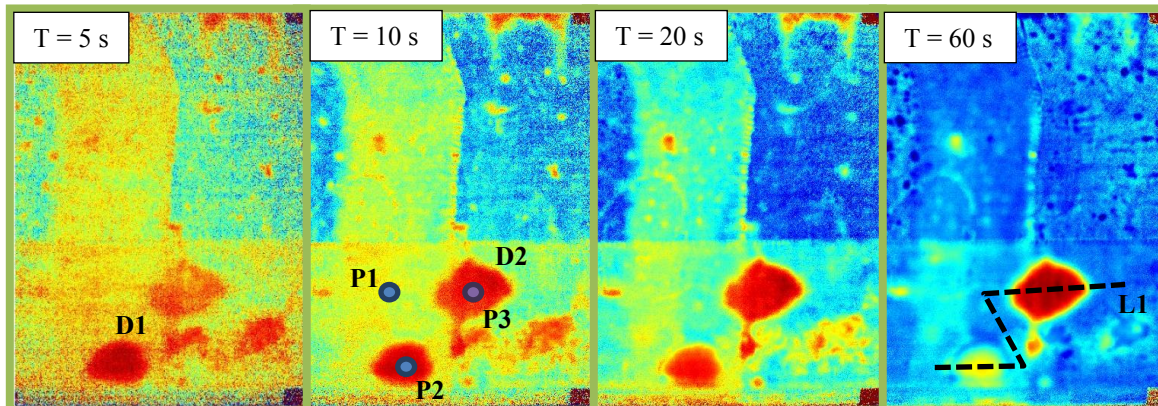


Figure 7. Pulse Phase images for Zone 2 (west side of Beam 1). Period, T , is equal to the inverse of the corresponding frequency from the discrete Fourier transform. Additional data for profile line, L1, and Points P1, P2, and P3 are provided in Figure 8.

Data was obtained for defects that occur at different depths in the FRP system for Zone 2. The defect that was closer to the surface, D1, did appear in the low-period image while the deeper defect, D2, developed a stronger defect signal strength as the period increased. A key observation was that the overall image quality and signal to noise ratio were not as high for the low-period PPT images. The Lock-in Thermography image obtained for $T = 5s$ provided a much clearer image of Defect D1 than the $T = 5s$ PPT image.

The complete phase angle vs. frequency plot for select points in Zone 2 is provided in Figure 8. Point P1 represents a defect-free region while P2 and P3 were located above Defect D1 and D2, respectively. A common method for extracting defect depth involves first determining the blind frequency, or the frequency at which a defect first appears in the series of phase images. The blind frequency for D1 was estimated to be 0.667 Hz ($T = 1.5s$). The blind frequency

for Defect D2 was more difficult to extract and the defect signal strength appeared to oscillate between frequency values of 0.45 Hz and 0.667 Hz ($T = 2.2$ s to $T = 1.5$ s). This highlights one potential pitfall associated with the PPT method. If the surface heating occurs over a longer period of time, such that defects are already visible in the thermal images at the end of heating, extracting the blind frequency is difficult. It is also necessary to develop a unique model for a specific heat pulse duration that relates blind frequency to depth.

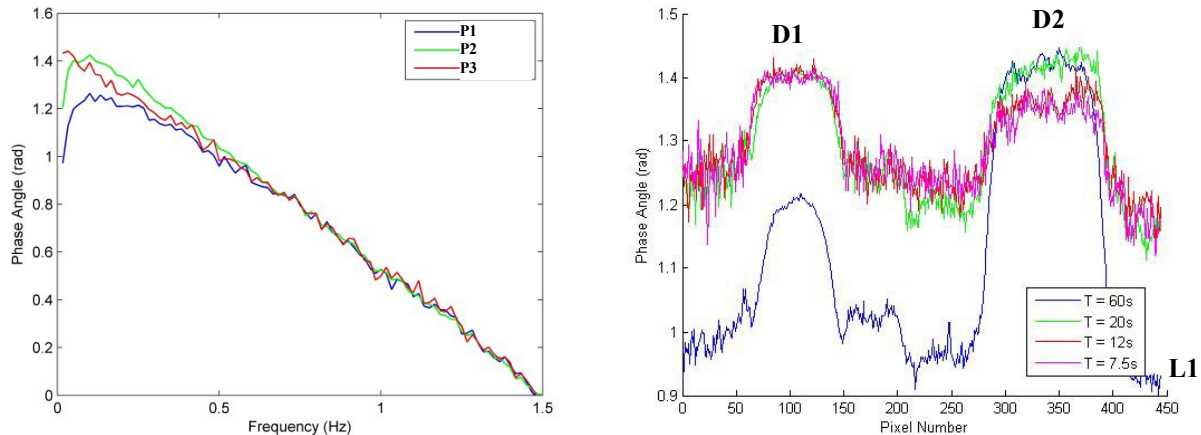


Figure 8. Phase angle data for defect and defect-free regions in Zone 2

4. CONCLUSIONS

This research explored different heating profiles and data processing techniques for the infrared thermography inspection of FRP composite systems used to strengthen reinforced concrete structures. The lock-in thermography approach provided a clear, albeit somewhat qualitative, method for determining the depth at which a defect exists beneath the surface of the FRP composite. The primary advantage of this method is that large areas can be inspected during a single observation period with relatively inexpensive heat sources. One downside to this method is that different FRP systems will require different heating periods in order to determine defect depth. If information about the specific FRP system is unknown, some degree of trial and error will also be necessary to determine the appropriate heating periods.

The pulse-phase thermography method provided reliable defect detection. The general trend between defect depth and blind frequency was observed, but the longer heating period of 30 sec (as opposed to flash heating) made precise identification of the blind frequency difficult. Additional research investigating step heating with normalization is currently underway that may provide an acceptable alternative to the lock-in and PPT methods.

5. ACKNOWLEDGEMENTS

The authors would like to thank Jovan Tatar and Dr. Trey Hamilton of the University of Florida for their contributions to this research effort. The assistance of Mr. David Wagner of the Florida Department of Transportation Structures Research Lab in Tallahassee, Florida, is also gratefully acknowledged.

6. REFERENCES

1. 60 Minutes. Falling apart: America's neglected infrastructure. Retrieved from <http://www.cbsnews.com/news/falling-apart-america-neglected-infrastructure/>
2. Federal Highway Administration. Deficient bridges by state and highway system 2014. Retrieved from <http://www.fhwa.dot.gov/bridge/nbi/no10/defbr14.cfm>

3. Mirmiran, A., Shahawy, M., Nanni, A., and Kharbari, V. (2004). NCHRP Report 514 – Bonded Repair and Retrofit of Concrete Structures Using FRP Composites.
4. American Concrete Institute (ACI) Committee 440 (2008). “Guide for the design and construction of externally bonded FRP systems for strengthening concrete structures.” American Concrete Institute, ACI 440.2R-08, Farmington Hills, Michigan.
5. ICC Evaluation Services (2003) “Acceptance criteria for concrete and unreinforced masonry strengthening using fiber-reinforced composite systems.” AC125, Whittier, California.
6. Brown, J. R., & Hamilton, H. R. (2007). Heating methods and detection limits for infrared thermography inspection of fiber-reinforced polymer composites. *ACI Materials Journal*, 104(5), 481-490.
7. Brown, J. R., & Hamilton, H. R. (2013). Quantitative infrared thermography inspection for FRP applied to concrete using single pixel analysis. *Construction and Building Materials*, 38, 1292-1302.
8. Ekenel, M., & Myers, J. J. (2007). Nondestructive evaluation of RC structures strengthened with FRP laminates containing near-surface defects in the form of delaminations. *Science and Engineering of Composite Materials*, 14(4), 299-315.
9. Ghiassi, B., Silva, S. M., Oliveira, D. V., Lourenço, P. B., & Bragança, L. (2014). FRP-to-masonry bond durability assessment with infrared thermography method. *Journal of Nondestructive Evaluation*, 33(3), 427-437.
10. Ghosh, K. K., & Karbhari, V. M. (2011). Use of infrared thermography for quantitative non-destructive evaluation in FRP strengthened bridge systems. *Materials and Structures*, 44(1), 169-185.
11. Mabry, N., K. Peters and R. Seracino (2015). Depth Detection of Bond Defects in Multilayered Externally Bonded CFRP-to-Concrete using Pulse Phase Thermography. *Journal of Composites for Construction*.